Inverting airborne geophysical data for mega-cell and giga-cell 3D Earth models

Glenn A. Wilson and Leif H. Cox, TechnoImaging
Martin Čuma and Michael S. Zhdanov, University of Utah and TechnoImaging

Today's mineral exploration is driven by the simple fact that discovery rates have not kept pace with the depletion of existing reserves. To improve discovery rates, there is an industry-wide consensus on the need to increase the "discovery space" by exploring under cover and to greater depths. This attracts increased risks which may be mitigated by improved targeting. To do this, mining geophysics needs to shift toward 3D geological models founded upon improved petrophysical understanding and geophysical inversion. Regardless of the inversion methodology used, all geological constraints manifest themselves in the user's prejudice of an a priori model, upper and lower bounds, and choice of regularization. However, the practice of geologically constrained inversion is not the major problem needing to be addressed. It is known (and accepted) that geology is inherently 3D, and is a result of complex, overlapping processes related to genesis, metamorphism, deformation, alteration and/or weathering. Yet, the mining geophysics community to date has not fully accepted that geophysics should also be 3D, and most often relies on qualitative analysis, 1D inversion, and deposit-scale 2D or 3D inversion. There are many reasons for this unfortunate deficiency, not the least of which has been the lack of capacity of existing 3D inversion algorithms. To date, these have not been able to invert entire surveys with sufficient resolution in sufficient time to practically affect exploration decisions.

This problem is most critical for airborne geophysical surveys which typically contain hundreds-to-thousands of line kilometers of multichannel data recorded every few meters, and often covering hundreds-to-thousands of square kilometers. Given the variety of access, environmental, logistical and efficiency considerations, most exploration strategies rely on airborne geophysical surveys for both regional mapping and targeting. Globally, it is estimated that in excess of US $300 million is annually invested in airborne geophysical surveying. Yet, much of that data are not (and historically have not) been exploited to their full potential. This issue will become more only pronounced in the future as airborne geophysical systems are now being deployed with multiple sensors (e.g., Rajagopalan et al., 2007). For example, Fugro Airborne Surveys are now operating systems that simultaneously measure GPS position, LIDAR, radar altimetry, digital video, total magnetic intensity, gamma-ray spectroscopy, gravity gradiometry, and electromagnetics (e.g., MEGATEM, TEMPEST, RESOLVE).

The challenge for 3D inversion is to be able to process multiple geophysical data from actual airborne systems to construct 3D Earth models with appropriate levels of geological complexity in sufficient time to contribute to exploration-related decisions. This paper reviews recent paradigm changes in 3D airborne geophysical inversion, namely the introduction of a moving footprint for mega-cell 3D airborne electromagnetic (AEM) inversion, and massive parallelization for giga-cell 3D potential field inversion. We introduce the quantitative terms mega-cell for those 3D Earth models with millions of cells, and giga-cell for those 3D Earth models pushing a billion cells. This terminology is intended to avoid use of the rather vague term large-scale.

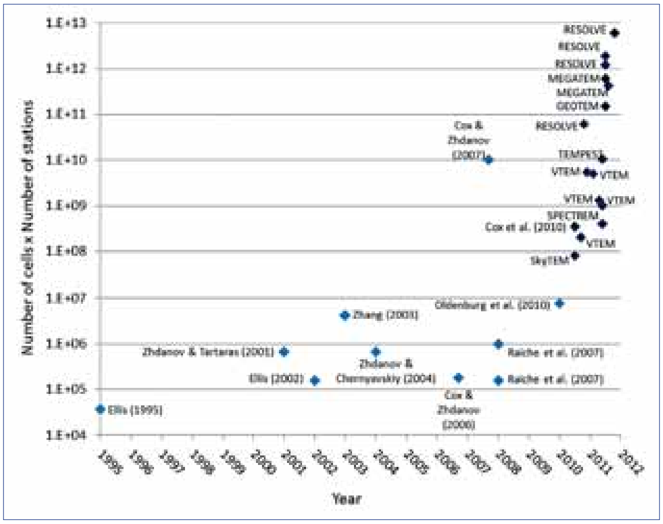

Figure 1. *A plot illustrating progress in 3D AEM inversion from 1995 to the present, summarized in terms of AEM problem size, i.e., number of cells in the 3D model times the number of transmitters in the survey, as extracted from published papers. The introduction of a moving footprint by Cox and Zhdanov (2007) that has been fully realized by Cox et al. (2010) has resulted in the paradigm change from kilo-cell to mega-cell 3D inversion for all AEM systems. Examples of different 3D AEM inversions completed by the authors are shown by black diamonds.*

From kilo-cell to mega-cell inversion

As recently as at the 2007 Decennial Mineral Exploration Conference, it was stated that "progress towards routine 2D and 3D inversions of AEM data has been slow, despite significant effort" (Macnae, 2007). This is, arguably, true, as Figure 1 effectively summarizes the history of 3D AEM inversion. As our pragmatic metric of measuring 3D AEM inversion capacity, we define the AEM problem size as the product of the number of cells in the 3D Earth model and the number of AEM stations modeled. While 3D modeling kernels have varied between authors, 3D AEM inversion has been limited to kilo-cell 3D models with tens to hundreds of stations. To be practical, it has been suggested that deposit-scale kilo-cell 3D inversions could be used for those parts of AEM surveys where 1D methods were deemed to have failed (e.g., Raiche et al., 2007). We again quote Macnae: "While the formal inversion process is practical for targets already identified as being of interest, it (3D inversion) is unlikely to be routine in the near future as a means of processing complete surveys." More recently, Yang and Oldenburg (2012) have suggested a workflow of randomly sampled data forming a grid of multiple subdomains ("tiles") that are independently inverted, and then postinversion stitching of those multiple "tiles" into a single 3D model. However, this approach still has an inherent problem of how to best stitch different "tiles" together.

Cox and Zhdanov (2006) used a combination of rigorous 3D modeling for the AEM responses, and linearized (QL) approximations for the AEM sensitivities. Cox and Zhdanov (2007) used the same combination of rigorous modeling and QL approximations, but introduced the concept of a moving footprint. According to this concept, one needs only to calculate the responses and sensitivities for that part of the 3D Earth model that is within the AEM system's footprint, and then superimpose the sensitivities for all footprints into a single, sparse sensitivity matrix for the entire 3D Earth model. By doing so, Cox and Zhdanov (2007) were able to increase the AEM problem size by nearly five orders of magnitude without dividing the inversion domain into smaller subdomains. This clearly represented a paradigm change in 3D AEM inversion methodology. Using the same moving footprint methodology, Cox et al. (2010) used rigorous modeling for both the AEM responses and their sensitivities. As shown by the black diamonds in Figure 1, this has made it practical to rigorously invert entire surveys with thousands of line kilometers of AEM data to mega-cell 3D models in hours using multiprocessor workstations.

We illustrate this progress with an example from the Kamiskotia area in Ontario, Canada, where numerous Cu-Zn volcanogenic massive sulfide (VMS) deposits were discovered. The Kamiskotia Volcanic Complex forms part of an Upper Archean volcanic succession of the Abitibi greenstone belt. Many of the VMS deposits occur along a single stratigraphic horizon at or near the sea floor close to inferred synvolcanic faults. It has been suggested that future exploration is best focused on extensions of the complex, and on those areas close to intersections of synvolcanic faults, with potential targets consisting of mafic and felsic volcaniclastic strata which can be replaced by VMS mineralization, and felsic facies flows and/or domes (Hathway et al., 2008).

To stimulate exploration for a depleting resource base, the Ontario Geological Survey initiated the Discover Abitibi Initiative in 1999 as a multiyear precompetitive exploration program for the western Abitibi greenstone belt. As part of this initiative, Fugro Airborne Surveys acquired 3729 line km of MEGATEM II airborne electromagnetic and magnetic data covering over 1500 km^2 of the Kamiskotia area during 2003. The survey was flown at 150-m line spacing with 200-m tie lines and nominal 120-m topographic drape. The MEGATEM II system was configured with a 90-Hz base frequency half-sine transmitter waveform recording 5 on-time and 15 off-time channels of inline and vertical dB/dt components in a receiver nominally towed 128 m behind and 50 m below

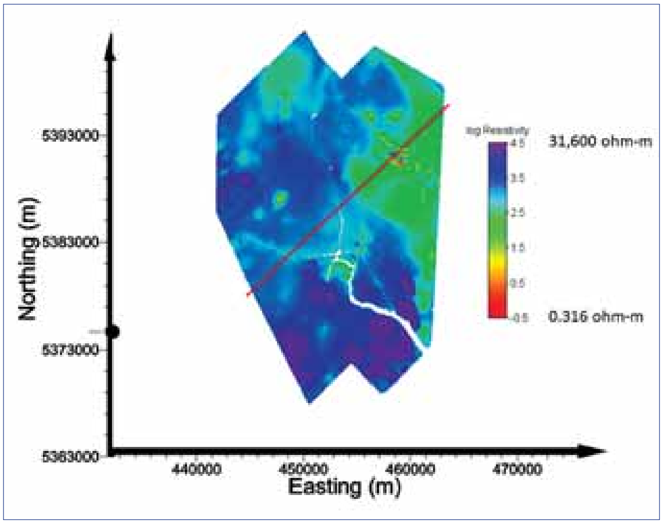

Figure 2. Horizontal cross section of resistivity at 150 m depth as extracted from the 3D model obtained from inversion of all 3729 line km of the Kamiskotia MEGATEM II dB/dt data. Line 3101 is shown by the red line (see Figure 4). Several VMS deposits occur within the survey area.

the transmitter. The data were processed and delivered to the Ontario Geological Survey as per the standard workflows of Fugro Airborne Surveys.

During 2011, we applied the AEM inversion method described above to all 3729 line km of MEGATEM II dB/dt data (approximately 3 million independent data) and produced a 3D resistivity model with over 15 million cells of 50 × 50-m horizontal discretization, and variable vertical discretization. The inversion commenced with no a priori model other than initial variable background representing the regional resistivity trend, and was completed within two days on a single node with eight 2.33 GHz cores and 196 GB memory. Figure 2 illustrates a horizontal depth section from the 3D resistivity model obtained from our 3D inversion. It is possible to identify regional geological trends consistent with the surface geology. However, at this scale, the model fidelity is not readily apparent. Figure 3 illustrates the superposition of the surface geology of a major intrusive unit (after Hathway et al., 2008) on a horizontal depth section from the 3D resistivity model we obtained from our 3D inversion. Subtle geological structures, such as faults, can be identified in the 3D resistivity model. Figure 4 is a vertical cross section through the same intrusive unit, and shows that the northeast dip was also recovered. In terms of potential VMS targets, several discrete conductive anomalies occur along the same stratigraphic horizon as the past producing VMS deposits. These are currently the subject of ongoing exploration.

From mega-cell to giga-cell inversion

Potential field data are the basis of most exploration strategies. Yet, relative to the volumes of potential field data acquired each year, very few 3D inversions are actually performed. Figure 5 effectively summarizes the history of 3D potential field inversions. We use the number of cells in a 3D model as the metric of 3D potential field inversion capacity.

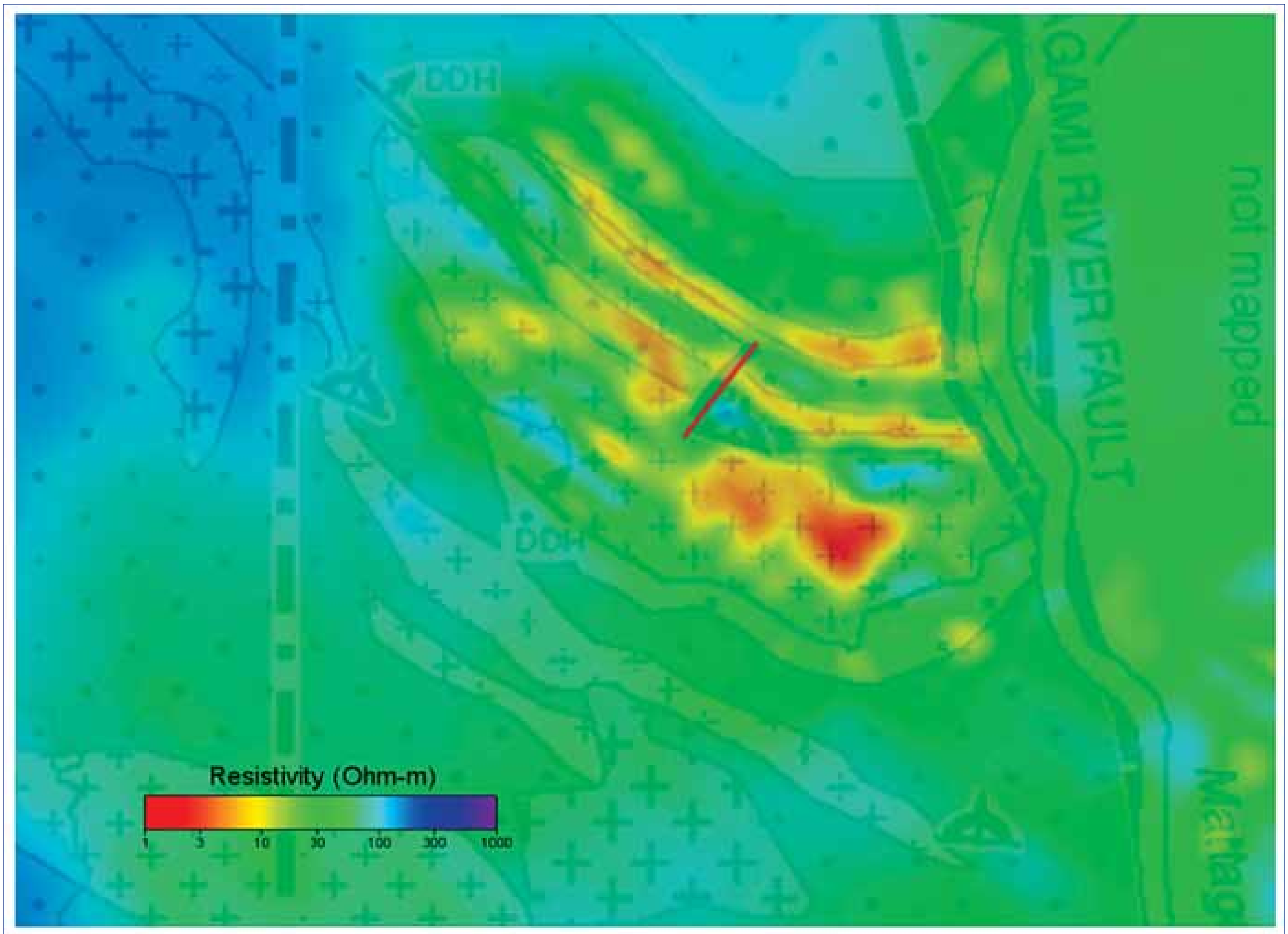

Figure 3. *Horizontal cross section of resistivity over an intrusive unit at 150 m depth, as extracted from the Kamiskotia 3D MEGATEM inversion model, superimposed on the surface geology (after Hathway et al., 2008). Note the discontinuities in the conductive units correlate with the known faults.*

In practice, large airborne surveys are usually divided into subsets (circa 1–3 million cells each), each of which is inverted with the resulting 3D Earth models stitched together postinversion. This reflects the current capacity of existing 3D inversion algorithms. Arguably, practical improvements in problem size over time can largely be attributed to Moore's law of computing power. To highlight this, we have shown the increase in computer memory (a valid proxy for computer power) over the same time (red line in Figure 5).

This problem can be rectified using the same moving footprint concept that we developed for 3D AEM inversion (Čuma et al., 2012). Indeed, potential-field sensors have a limited spatial sensitivity. Therefore, one needs only to calculate the responses and sensitivities for that part of the 3D Earth model that is within a given sensor's sensitivity, and then superimpose those sensitivities for all footprints within a single sensitivity matrix for the entire 3D Earth model. Unlike electromagnetics, the inversion of potential fields is a linear inverse problem which results in increased computational efficiency. We have implemented this moving footprint approach, along with a massive parallelization of the software which exhibits linear strong and weak scaling (e.g., Wilson et al., 2011). As shown by the black diamonds in Figure 5, this has made it practical for us to invert entire potential field surveys to giga-cell 3D models in a day using moderate cluster resources. Relative to other software, we have increased the potential field problem size by several orders of magnitude. In practice, this means we can now invert entire surveys for deposit-scale resolution.

We illustrate this progress with an example from the Bathurst Mining Camp in New Brunswick, Canada, where at least 35 Pb-Zn-Cu-Ag type VMS deposits and over 100 known mineral occurrences have been discovered since the early 1950s. The camp is part of the northern Miramichi Highlands, and is divided into three groups: Miramichi, Tetagouche, and Fournier. The Miramichi Group is composed of quartz-rich sandstone, shale, quartz-wacke, and black shale. The Tetagouche Group is divided into three formations. The Boucher Brook Formation consists of two units, one composed of shales and sandstones, and the other composed of basalts. The Flat Landing Brook Formation consists of felsic volcanic rocks. The Nepisiguit Falls Formation consists of quartz and feldspar crystal-rich volcaniclastics and volcanics, and fine-grained sedimentary rocks. The Fournier Group is

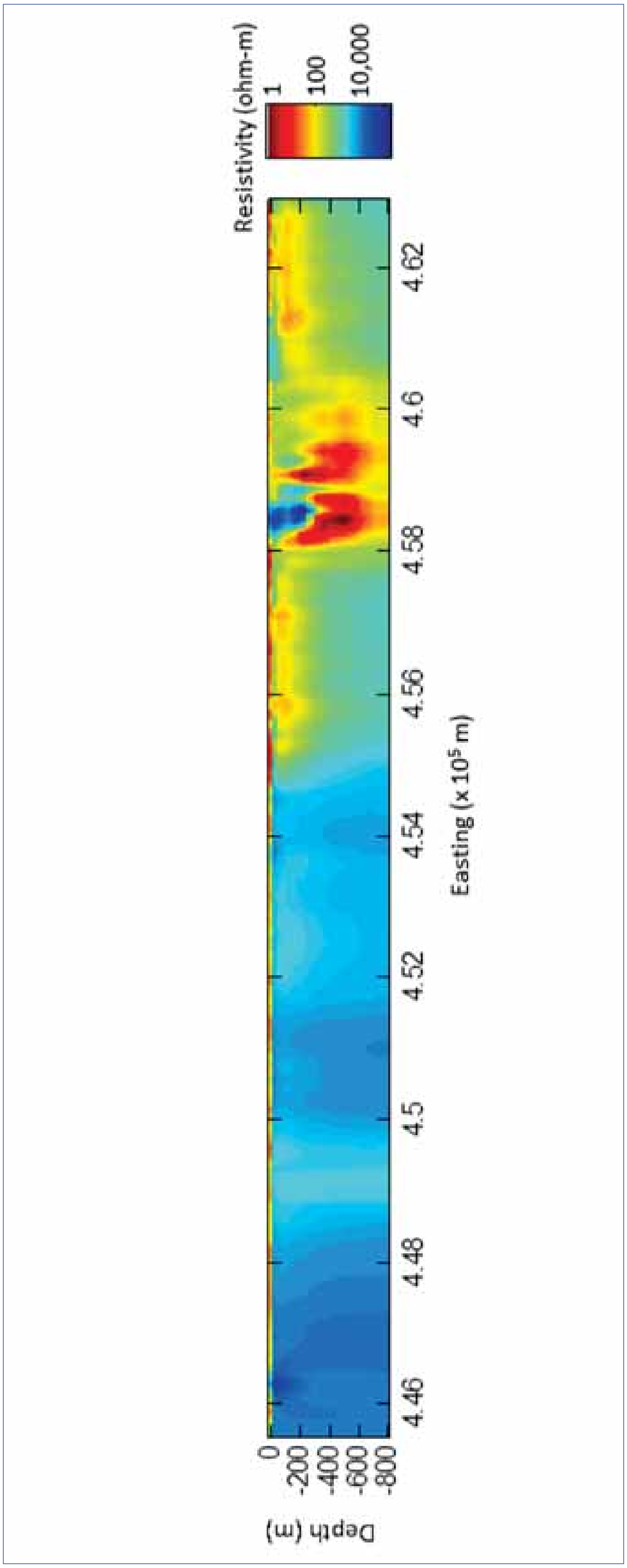

Figure 4. *Vertical cross section (red lines on depth slices in figures 2 and 3) of resistivity as extracted from MEGATEM line 3101 that crosses the conductive intrusive units shown in Figure 3. The overburden is recovered as a variably thin but conductive layer. Note the direction of the dip on the conductive units correlates with those in the surface geology shown in Figure 3.*

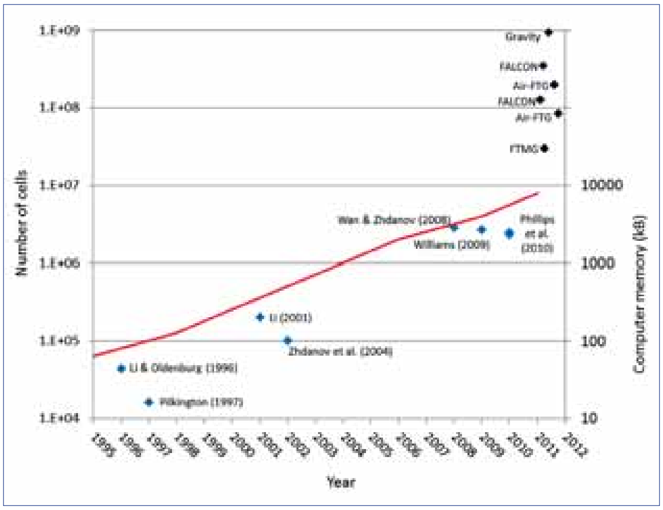

Figure 5. *A plot illustrating progress in 3D potential field inversion from 1995 to the present, summarized in terms of number of cells in the 3D model, as extracted from published papers. For comparison, available desktop computer memory is also shown (Source = Intel). Note that the increase in 3D model size trends directly with desktop computing memory (red line). The introduction of a moving footprint and massively parallel inversion by the authors has resulted in the paradigm change from mega-cell to giga-cell 3D inversion for all types of potential fields. Examples of different 3D potential field inversions completed by the authors are shown by black diamonds.*

composed of thickly bedded shales, lithic wacke, and basalt.

The structural geology of the camp is complex, with five groups of folds identified. It has been suggested that most of the Tetagouche volcanic rocks are of basin-margin origin, deposited on a rifting continental crust. It follows that many of the VMS deposits are associated with tuffite and silicic volcanic rocks of the Nepisiguit Falls and Flat Landing Brook formations of the Tetagouche Group (Van Staal, 1992; Lentz, 1999). Typically, the VMS deposits have a density of about 4 g/cc, whereas the host rocks (sediments, felsic tuffs, or their metamorphic equivalents) have densities between 2.7 and 2.8 g/cc (Dransfield et al., 2001).

On behalf of Nordanda (now Xstrata), SLAM Exploration, and the Government of New Brusnwick, Bell Geospace acquired 15,500 line km of Air-FTG full-tensor gravity gradiometry data that covered more than 2755 km^2 of the camp during 2004. The survey was flown at 200-m line spacing with 2000-m tie lines and 80-m topographic drape. Bell Geospace subsequently reprocessed the Air-FTG data during 2010 using improved terrain correction, leveling, automatic tilt, and full-tensor noise reduction (FTNR).

In 2011, we inverted all 15,500 line km of 2.70 g/cc terrain-corrected FTNR Air-FTG data (approximately 1.4 million independent data) to an SRTM-derived topographic conforming 3D density model with over 85 million cells of 50 × 50 × 25 m resolution. The inversion commenced with no a priori model, and was completed within one day on 16 nodes, each with eight 2.67 GHz cores and 24 GB of memory. Figure 6 illustrates a horizontal depth section from the 3D density contrast model obtained from our 3D inversion, overlain with the surface geology of Lentz (1999). It is pos-

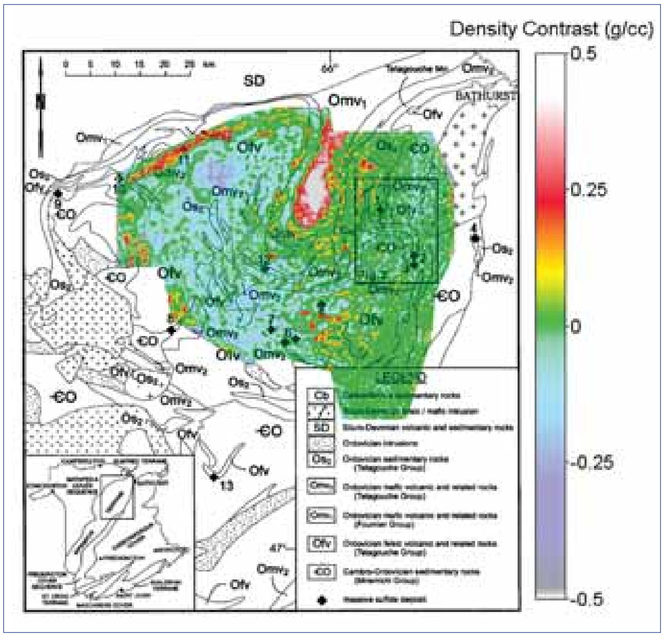

Figure 6. *Horizontal cross section of density contrasts (relative to 2.70 g/cc) at 150 m depth as extracted from the 3D model obtained from inversion of all 15,500 line km of the Bathurst Mining Camp Air-FTG data, superimposed on the surface geology (after Lentz, 1999). The Brunswick Belt is shown by the black box.*

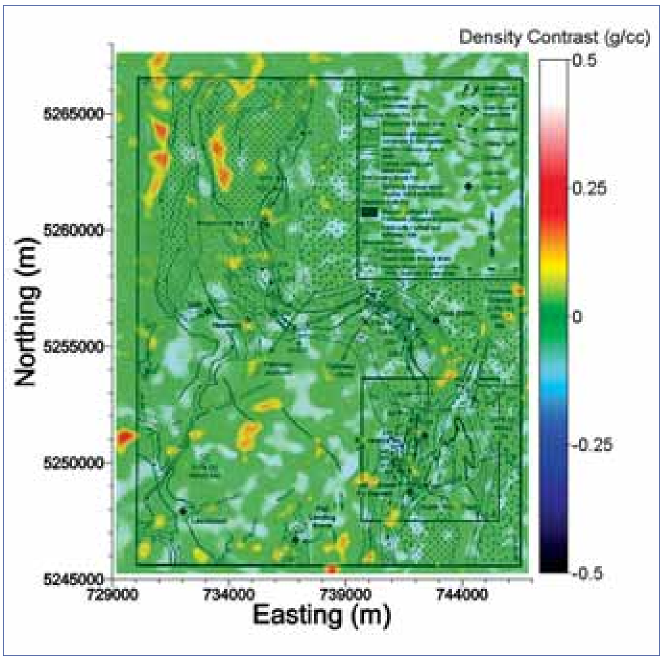

Figure 7. *Horizontal cross section of density contrasts (relative to 2.70 g/cc) of the Brunswick Belt at 50 m depth as extracted from the 3D model obtained from inversion of all 15,500 line km of the Bathurst Mining Camp Air-FTG data, superimposed on the surface geology (after Lentz, 1999). Note the positive density contrasts associated with many of the known mines in the district. Several unidentified anomalies are associated with the same stratigraphic horizon, and represent potential VMS targets.*

sible to identify regional geological trends consistent with the surface geology. However, at this scale, the model fidelity is again not readily apparent—particularly for targeting VMS deposits. Figure 7 illustrates the superposition of the surface geology from the Brunswick Belt (after Lentz) on a horizontal depth section from the 3D density contrast model obtained from our 3D inversion. In terms of potential VMS targets, it is readily seen that several discrete density anomalies not mapped by Lentz occur along the same stratigraphic horizon as the past and present producing VMS deposits. These are currently the subject of ongoing exploration.

And beyond

The paradigm changes in 3D AEM and potential field inversions presented in this paper have been driven by algorithmic improvements coupled with parallel computing. We are continuing to develop new modeling and inversion algorithms for implementation on existing and future parallel computing platforms. The capacity of these methods to invert airborne geophysical data quicker than it can be acquired provides new opportunities for real-time 3D imaging and quality control. With the emergence of multisensor airborne systems, the 3D inversion capabilities discussed provide the basis of multimodal 3D joint inversion, and this will constitute the goal of future research.

Conclusions

Today's mineral exploration is driven by the simple fact that discovery rates have not kept pace with the depletion of existing reserves in response to increasing consumption. Airborne geophysics will continue to be an essential component of any mineral exploration strategy, whether for regional mapping or targeting. Yet, despite improvements in airborne geophysical acquisition and processing technologies, interpretation has historically lagged by at least a decade. In this paper, we have identified those recent paradigm changes that have had immediate and significant impacts on mineral exploration; namely the introduction of a moving footprint for mega-cell 3D AEM inversion, and massive parallelization for giga-cell 3D potential field inversion. For the first time, it is now practical to reliably invert entire airborne geophysical surveys in 3D with deposit-scale resolution quicker than that data can be acquired. This capability to quantitatively interpret airborne geophysical data in 3D will continue to lead to improved understanding and targeting of mineralization systems (e.g., Combrinck et al., 2012; Pare et al., 2012). **TLE**

References

Combrinck, M., L. H. Cox, G. A. Wilson, and M. S. Zhdanov, 2012, 3D VTEM inversion for delineating sub-vertical shear zones in the West African gold belt: Presented at ASEG 22nd Geophysical Conference and Exhibition, Brisbane.

Cox, L. H. and M. S. Zhdanov, 2006, Rapid and rigorous 3D inversion of airborne electromagnetic data: 76th Annual International Meeting, SEG, Expanded Abstracts, 795–798.

Cox, L. H. and M. S. Zhdanov, 2007, Large-scale 3D inversion of HEM data using a moving footprint: 77th Annual International Meeting, SEG, Expanded Abstracts, 467–470.

Cox, L. H., G. A. Wilson, and M. S. Zhdanov, 2010, 3D inversion of airborne electromagnetic data using a moving footprint: Exploration Geophysics, **41**, no. 4, 250–259, doi:10.1071/EG10003.

Čuma, M., G. A. Wilson, and M. S. Zhdanov, 2012, Large-scale 3D inversion of potential field data: Geophysical Prospecting, **60**, doi: 10.1111/j.1365-2478.2011.01052.x.

Dransfield, M., A. Christensen, M. Rose, P. Stone, and P. Diorio, 2001, FALCON test results from the Bathurst Mining Camp: Exploration Geophysics, **32**, no. 4, 243–246, doi:10.1071/EG01243.

Hathway, B., G. Hudak, and M. A. Hamilton, 2008, Geological setting of volcanic-associated massive sulphide deposits in the Kamiskotia area, Abitibi Subprovince, Canada: Economic Geology and the Bulletin of the Society of Economic Geologists, **103**, no. 6, 1185–1202, doi:10.2113/gsecongeo.103.6.1185.

Lentz, D. R., 1999, Petrology, geochemistry, and oxygen isotope interpretation of felsic volcanic and related rocks hosting the Brunswick 6 and 12 massive sulfide deposits (Brunswick Belt), Bathurst Mining Camp, New Brunswick, Canada: Economic Geology and the Bulletin of the Society of Economic Geologists, **94**, no. 1, 57–86, doi:10.2113/gsecongeo.94.1.57.

Macnae, J., 2007, Developments in broadband airborne electromagnetics in the past decade: in B. Milkereit, ed., Proceedings of Exploration 07: Fifth Decennial International Conference on Mineral Exploration, 387–398.

Pare, P., A. V. Gribenko, L. H. Cox, M. Čuma, G. A. Wilson, M. S. Zhdanov, J. Legault, J. Smit, and L. Polomé, 2012, 3D inversion of SPECTREM and ZTEM data from the Pebble Cu-Au-Mo porphyry deposit, Alaska: Presented at ASEG 22nd Geophysical Conference and Exhibition, Brisbane.

Raiche, A., F. Sugeng, and G. Wilson, 2007, Practical 3D EM inversion–P223F software suite: Presented at ASEG 19th Geophysical Conference and Exhibition, Perth.

Rajagopalan, S., J. Carlson, and D. Wituik, 2007, Kimberlite exploration using integrated airborne geophysics: Presented at ASEG 19th Geophysical Conference and Exhibition, Perth.

van Staal, C. R., 1992, The Ordovician Tetagouche Group, Bathurst camp, northern New Brunswick, Canada: History, tectonic setting, and distribution of massive sulfide deposits: Exploration and Mining Geology, 1, 93–103.

Wilson, G. A., M. Čuma, and M. S. Zhdanov, 2011, Massively parallel 3D inversion of gravity and gravity gradiometry data: Preview, 152, 29–34.

Yang, D. and D. W. Oldenburg, 2012, Practical 3D inversion of large airborne time domain electromagnetic data sets: Presented at ASEG 22nd Geophysical Conference and Exhibition, Brisbane.

Acknowledgments: The authors acknowledge TechnoImaging for permission to publish. M. Čuma and M. S. Zhdanov acknowledge support from the University of Utah's Consortium for Electromagnetic Modeling and Inversion (CEMI) and Center for High Performance Computing (CHPC). Fugro Airborne Surveys is acknowledged for assistance with the Kamiskotia MEGATEM data released by the Ontario Geological Survey. Bell Geospace is acknowledged for assistance with the Bathurst Mining Camp Air-FTG data released by the Department of Natural Resources of the Government of New Brunswick.

Corresponding author: glenn@technoimaging.com